

Hybrid model for the damped transient response of giant dipole resonances

A. P. Severyukhin ^{1,2} S. Åberg ³ N. N. Arsenyev ¹ and R. G. Nazmitdinov ^{1,2,*}

¹*Bogoliubov Laboratory of Theoretical Physics, Joint Institute for Nuclear Research, 141980 Dubna, Moscow Region, Russia*

²*Dubna State University, 141982 Dubna, Moscow Region, Russia*

³*Mathematical Physics, Lund University, P.O. Box 118, S-22100 Lund, Sweden*



(Received 19 April 2021; accepted 8 October 2021; published 21 October 2021)

We suggest the hybrid model for the description of the dipole spreading widths, in which the strength function is built on the one-phonon strength distribution folded with the energy-dependent Lorentzian. Its energy dependence is brought about by (i) the energy-dependent smearing parameter and (ii) the energy-dependent shift of the one-phonon states. These variables are estimated by means of the two-phonon density, provided by a modified Fermi gas model with uniformly spaced states, and with the aid of the weak constant interaction between the one-phonon states and the two-phonon states, considered as background states. Based on calculated one-phonon states, the model is analytically solvable. To explore the validity of the model we analyze the properties of the 1^- spectrum in ^{206}Hg , ^{206}Pb , and ^{210}Po nuclei. Our results demonstrate that the description of the decay widths within the latter approach is in good agreement with that obtained in the quasiparticle random phase approximation, by means of the random distribution of the coupling between microscopic one-phonon states and two-phonon states, generated by the Gaussian orthogonal ensemble distribution.

DOI: [10.1103/PhysRevC.104.044327](https://doi.org/10.1103/PhysRevC.104.044327)

I. INTRODUCTION

Nowadays, various nuclear reaction and nuclear structure studies have become high demand fields for analysis of stellar structure, stellar evolution, and nucleosynthesis applications (e.g., Ref. [1]). These studies provide important constraints for the equation of state of neutron-rich matter, which is important for an understanding of the formation of neutron stars [2] and core-collapse supernovas [3]. Among many considered phenomena the analysis of photon interactions with nuclei provides as well important information on stellar star formation rate and on the nuclear equation of state (see, for example, Ref. [4]). Although there are phenomenological models employed for the latter analysis, there is a need for a simple but reliable microscopic model of the nuclear response to an electromagnetic radiation. In this way we can establish the consistency between nuclear structure theory and heuristic assumptions in stellar physics.

In nuclear structure the response of a nucleus to an electromagnetic probe is provided by strength functions that describe the photoexcitation as well as the deexcitation of a nucleus by means of γ radiation. In fact, the strength function is a synergy product of the theoretical modeling of nuclear reactions and nuclear structure dynamics. It is based on the assumption that the nuclear level density is high enough at high excitation energies, and, therefore, the nuclear decay properties can be described statistically [5]. In particular, in the energy region of 10–20 MeV reaction theory correlates the strength function with the photoabsorption cross section, dominated by

the electric dipole ($E1$) radiation. This region characterizes the properties of the giant dipole resonance (GDR), treated in nuclear structure theory as a collective coherent motion of protons against neutrons.

Starting from a seminal paper of Migdal [6], there is a vast literature devoted to numerous attempts to describe spectral as well as decay properties of the GDR consistently (see for a review Refs. [7–13] and references therein). Various microscopic approaches circumscribe quite well the centroid energy, operating on the premise that the GDR is essentially excited by an external field through a one-body interaction. Another important characteristic that provides valuable information on the excitation and decay of the GDR is its width Γ . There is a consensus that any giant resonance width consists of the contribution of Landau damping Γ_L , an escape width Γ^\uparrow , and a spreading width Γ^\downarrow , i.e., $\Gamma = \Gamma_L + \Gamma^\uparrow + \Gamma^\downarrow$. The Landau damping is responsible for the fragmentation of the initial excitation into one-particle–one-hole ($1p-1h$) states serving as doorway states; a direct particle emission gives rise to an escape width; and the decay evolution of the doorway states along the hierarchy of more complicated ($2p-2h$, $3p-3h$, etc.) configurations to compound states determines a spreading width. An understanding of spreading widths associated with the cascade of couplings and their fragmentations due to these couplings (see Refs. [14–16]) remains an open fundamental problem for microscopic approaches. Evidently, the insurmountable obstacle is the existence of many degrees of freedom for a many-body quantum system.

According to a general wisdom, the one-particle continuum and, at least, $2p-2h$ configurations coupled to the random phase approximation (RPA) phonons are imperative elements for the microscopic description of the GDR width. At these

*rashid@theor.jinr.ru

conditions the escape width Γ^\uparrow is important for the interpretation of the total width in light and exotic nuclei (see Refs. [17–19]). However, for intermediate and heavy nuclei the contribution of Γ^\uparrow to the total width is small and can be ignored. Among acceptable approximations to the problem of the GDR width in heavy nuclei within microscopic approaches is omitting from consideration the escape width (Γ^\uparrow) in calculations. We recall that, in contrast to spherical nuclei, in deformed nuclei the experimental widths are systematically larger, and may develop a two- or three-peak structure. In this paper we consider only spherical or near-spherical nuclei around ^{208}Pb and focus our attention on the decay width $\Gamma \approx \Gamma_L + \Gamma^\downarrow$.

To carry out our study we employ the quasiparticle random phase approximation (QRPA) with Skyrme interactions in a separable approximation [20,21]. Hereafter, we use the parameter set of SLy4 [22], which is adjusted to reproduce the nuclear matter properties, as well as nuclei charge radii, binding energies of doubly magic nuclei. Making use of the finite rank separable approximation [20] for the residual interaction enables us to perform QRPA calculations in very large two-quasiparticle spaces. In particular, the cutoff of the discretized continuous part of the single-particle spectra is at the energy of 100 MeV. Following the basic ideas of the quasiparticle-phonon model [9], the Hamiltonian is then diagonalized in a space spanned by states composed of one and two QRPA phonons [23,24].

It was shown recently that the microscopic phonon-phonon coupling (PPC) describes reasonably well the gross structure of spreading widths of giant monopole, dipole, and quadrupole resonances in the doubly magic heavy nuclei [25]. Further, the comparison of the microscopic results with those obtained by means of the random coupling of the one-phonon with the two-phonon states established a good correspondence between the two approaches. We named the approach based on the random coupling as the damped transient response. Within this approach, the description of the GDR spreading widths, calculated for a few nuclei around ^{208}Pb , demonstrates again a close similarity with those obtained with the aid of the microscopic PPC [26].

The purpose of the present paper is twofold: first, to develop a model that simplifies the calculations of the GDR spreading width, and relies only on one-phonon states, calculated microscopically; second, to demonstrate that this model can be successfully implemented for the description of the damped transient response of the GDR in heavy nuclei, providing a reliable approximation of the PPC approach.

II. PRELIMINARIES

The experimental systematics for spherical as well as deformed nuclei in the $150 < A < 190$ and $220 < A < 253$ ranges provides the following estimation for the GDR centroid energy [12,27]:

$$E_c = e_1(1 - I^2)^{1/2} \frac{A^{-1/3}}{[1 + e_2 A^{-1/3}]^{1/2}}, \quad (1)$$

where $e_1 = 128.0 \pm 0.9$ MeV, $e_2 = 8.5 \pm 0.2$, and $I = (N - Z)/(N + Z)$. The GDR width is estimated from a simple

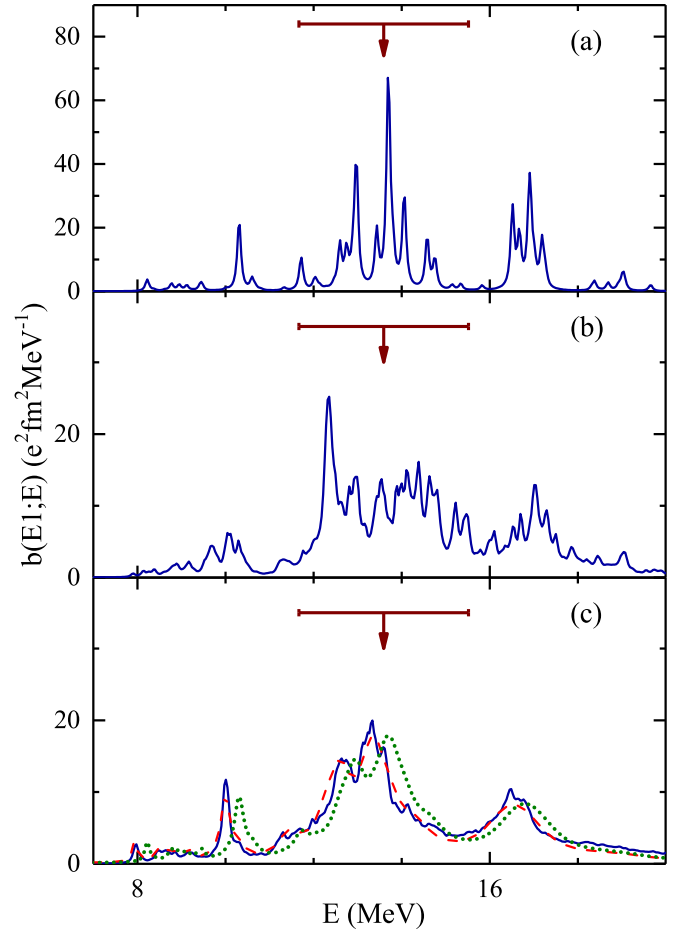


FIG. 1. Comparison of the results for the dipole strength distribution for ^{208}Pb , obtained by means of (a) the one-phonon approximation, (b) the PPC approach, and (c) the random coupling matrix elements between the one- and two-phonon configurations (the doorway model, solid line). The strength distributions are described by the Lorentzian function with the smoothing parameter of 100 keV. The results, based on the one-phonon approximation (the hybrid model), are connected by dotted and dashed lines [see panel (c)]. The dashed curve is associated with the results where the perturbation correction to the one-phonon energy, ΔE [Eq. (30)], is taken into account (see Sec. III B). The dotted line is associated with the results where $\Delta E = 0$. The experimental centroid and width of the GDR are 13.59 and 3.85 MeV [28], which are denoted by arrows and lines in panels (a)–(c), respectively.

power-law expression $\Gamma = cE_c^d$ with $c = 0.42 \pm 0.05$ MeV and $d = 0.90 \pm 0.04$.

Let us go briefly through the details of the microscopic approach. The calculated position of the resonance centroids E_c and the spreading width Γ have been defined with the aid of the energy-weighted moments $m_k = \int b(E1; E)E^k dE$: (i) $E_c = m_1/m_0$ and (ii) $\Gamma = 2.35\sqrt{m_2/m_0 - (m_1/m_0)^2}$ [29]. From our experience it is good enough to define the energy interval for location of the resonance width, taking 95% of the energy-weighted sum rule symmetrically around the centroid's position (E_c) (see details in Ref. [26]). A typical dipole strength distribution, obtained in the QRPA, is shown in Fig. 1(a). Hereafter, for the presentation of the strength

TABLE I. Centroid energies E_c and the spreading widths Γ of the GDR for ^{206}Hg , ^{206}Pb , and ^{210}Po nuclei. These characteristics, calculated in the energy region 9.5–18.5 MeV, are provided by the following approaches: (i) within the QRPA, (ii) by means of the PPC, (iii) employing the random distribution of coupling matrix elements (Random), and (iv) within the hybrid model (Hybrid). For comparison, we present as well the centroid energy and width values, given by the empirical systematics [12,27] (Syst.) and by available experimental data [28] (Expt).

	E_c (MeV)						Γ (MeV)					
	Expt.	Syst.	Theory				Expt.	Syst.	Theory			
			QRPA	PPC	Random	Hybrid			QRPA	PPC	Random	Hybrid
^{206}Hg		13.53	14.1	14.1	13.8	13.7		4.38	4.6	5.0	5.0	5.0
^{206}Pb	13.59	13.59	14.2	14.1	14.0	13.9	3.85	4.40	4.6	4.9	4.9	4.9
^{210}Po		13.54	14.2	14.1	13.9	13.8		4.38	4.7	4.9	5.0	5.0

distribution, described by the standard Lorentzian function (if not mentioned otherwise), we use the smoothing parameter 100 keV. It is nearby to the experimental resolution of the dipole strength distribution.

Using the QRPA basis, we consider the linear superposition of one-phonon and two-phonon configurations. This wave function of the 1^- states is constructed, taking into account all two-phonon terms that are built from the phonons with different multipolarities $I^\pi = 0^+, 1^-, 2^+, 3^-, 4^+$, coupled to the 1^- state. Considering the coupling between the one- and two-phonon configurations, we diagonalize the model Hamiltonian and obtain new states, described by a wave function which contains the mixture of one- and two-phonon configurations.

With the chosen set of multipolarities, the coupling (the PPC) of the one-phonon states with a complex background of two-phonon states yields a strong redistribution of the one-phonon dipole strength in the region of the GDR in the heavy spherical nucleus ^{208}Pb (see Fig. 1 in Ref. [25]), providing a good description of the experimental data. The coupling suppresses the double bump humping and pushes the high-lying one-phonon strength near ≈ 17 MeV down. As it was already mentioned in Ref. [30] the Skyrme forces do not possess the correct neutron-proton symmetry properties, and hence one could fit the parameters of phenomenological interactions to improve the description of the spreading width, additionally to the coupling of the RPA phonons with complex configurations. In particular, following a similar scenario, a good description of the spectral strength distribution for ^{208}Pb is obtained within the phonon-coupling model [18], where only collective phonons were used in the complex configurations. It is noteworthy that in our approach the RPA solutions, treated as quasibosons, consist of one-phonon states corresponding to collective GDR states, as well as of pure two-quasiparticle states, that contribute to the coupling on an equal footing. The inclusion of higher multipoles and magnetic phonons is highly likely to increase the fragmentation. However, the main aim of our paper is to provide an efficient approach that could supersede the cumbersome PPC calculations and might describe the GDR decay width on the same level of accuracy.

The obtained results [see Fig. 1(b)] demonstrate evidently two facts. First, the presence of the two-phonon components increases slightly the decay width value Γ in comparison with that obtained in the QRPA (see also Table I). We conclude

that the Landau damping is the basic mechanism of the decay in the considered case. Second, the influence of the PPC is much more prominent on the strength redistribution, which could be compared with a possible experimental dataset. The obtained results raise the reasonable question on the degree of the energy shift, produced by the presence of the two-phonon components. An additional question arises on the energy dependence of the smoothing parameter: does it depend on the excitation energy, or should it be a fitting constant in theoretical approaches? The underlying motivation for this question is the energy dependence of the resonance width in the phenomenological expression for the strength function (see, e.g., Sec. 4.2.1 in Ref. [12]).

III. SPREADING WIDTHS

To answer the above questions and to reach our announced aim, we recapitulate first our doorway model for the fragmentation.

A. Doorway model

Thus, we consider the Hamiltonian

$$H = H_d + H_b + V, \quad (2)$$

where the doorway Hamiltonian has the form

$$H_d = \sum_i^{N_d} \omega_i Q_i^+ Q_i. \quad (3)$$

Here, the energies ω_i are obtained from the microscopic QRPA calculations of the dipole phonon states $|d; \omega_i\rangle$; N_d one-phonon states constitute the doorway states. Transition matrix elements between the ground state and the one-phonon state are obtained from the QRPA calculation as

$$B_i = \langle d; \omega_i | \mathcal{M}_{1^-} | 0 \rangle, \quad (4)$$

where $|0\rangle$ is the QRPA ground state, and the operator \mathcal{M}_{1^-} is

$$\mathcal{M}_{1^-} = -\frac{Z}{A} e \sum_{k=1}^N r_k Y_{1\mu}(\hat{r}_k) + \frac{N}{A} e \sum_{k=1}^Z r_k Y_{1\mu}(\hat{r}_k). \quad (5)$$

Here, N , Z , and A are the neutron, proton, and mass numbers, respectively; r_k indicates the radial coordinate for neutrons (protons); and $Y_{1\mu}(\hat{r}_k)$ is the corresponding spherical harmonic. This definition of the dipole operator eliminates

contaminations of the physical response due to the spurious excitation of the center of mass.

The N_b background states are described by the Hamiltonian

$$H_b = \sum_k^{N_b} \Omega_k a_k^\dagger a_k, \quad (6)$$

with eigenstates $|b; \Omega_k\rangle$ and corresponding energies Ω_k . The number of background states is much larger than the number of doorway states, $N_b \gg N_d$. The $E1$ matrix element between the ground state and all background states is zero:

$$\langle b; \Omega_k | \mathcal{M}_{1^-} | 0 \rangle = 0. \quad (7)$$

We assume that there is no coupling between individual one-phonon states, and no coupling between the background states. The coupling, V , between the doorway (one-phonon) states $|d; \omega_i\rangle$, and the background states, $|b; \Omega_j\rangle$, is taken as

$$V = \sum_{i,k} V_{d_i, b_k} (Q_i^\dagger a_k + Q_i a_k^\dagger), \quad (8)$$

with

$$V_{d_i, b_k} = \langle d; \omega_i | V | b; \Omega_k \rangle, \quad (9)$$

and fulfilling

$$V_{d_i, b_k} = V_{b_k, d_i}. \quad (10)$$

We also assume that these coupling matrix elements can be replaced by a random interaction where the matrix elements, V_{d_i, b_k} , are Gaussian distributed random numbers,

$$P(V_{d_i, b_k}) = \frac{1}{\sigma \sqrt{2\pi}} \exp\left(-\frac{V_{d_i, b_k}^2}{2\sigma^2}\right), \quad (11)$$

with the width or strength

$$\sigma = \sqrt{\langle V_{d_i, b_k}^2 \rangle}. \quad (12)$$

Solving the eigenvalue problem for the total doorway Hamiltonian, Eq. (2), by a numerical diagonalization

$$H|\mu\rangle = E_\mu|\mu\rangle, \quad (13)$$

one obtains the total wave functions as a mixture between one-phonon states and background states:

$$|\mu\rangle = \sum_{i=1}^{N_d} c_i^\mu |d; \omega_i\rangle + \sum_{k=N_d+1}^N c_k^\mu |b; \Omega_k\rangle. \quad (14)$$

Such wave functions yield a fragmentation of the GDR strength on all N states, where $N=N_b + N_d$ is the total number of states considered in the model.

If there is no interaction between the one-phonon states and the background states ($\sigma=0$), the dipole strength distribution,

$$b^d(E1; E) = \sum_{i=1}^{N_d} |B_i|^2 \delta(E - E_i), \quad (15)$$

is concentrated on the one-phonon states. With the introduced coupling, the strength is spread over all $\mu = 1 \dots N$ states with

matrix elements given by

$$P_\mu = \langle \mu | \mathcal{M}_{1^-} | 0 \rangle = \sum_{i=1}^{N_d} c_i^\mu B_i, \quad (16)$$

where Eqs. (4) and (7) are used. The dipole strength distribution becomes

$$b(E1; E) = \sum_{\mu=1}^N |P_\mu|^2 \delta(E - E_\mu), \quad (17)$$

where $\delta(E - E_\mu)$ is replaced, for convenience, by the Lorentzian function with the smoothing parameter $\Delta = 100$ keV. The dipole strength distribution is finally averaged over ten realizations of the random interaction (see details in Ref. [26]). Figure 1(c) illustrates the result of the ensemble averaging. We recall that in this case the QRPA results are completed by the calculations in which the doorway one-phonon 1^- states interact randomly with the background two-phonon states, generated by the Gaussian orthogonal ensemble (GOE) distribution.

B. The hybrid model

In this section we introduce an analytical solvable model of the spreading width, Γ^\downarrow , in terms of mixing of the one-phonon dipole strength with complex background states. Next, by means of this width we aim to provide the dipole strength distribution that would supersede the PPC description.

Let us consider two-phonon states as our background states. The amplitudes c_i^μ describe the distribution of the properties of the one-phonon (doorway) states i over the spectrum E_μ [see Eqs. (13) and (14)]. As a result, the strength function (17) is defined by the matrix element (16) with the probability of the state $|d; \omega_i\rangle$ per unit energy interval of the spectrum E_μ , given by the Breit-Wigner function (see, e.g., Ref. [5]):

$$P_d(E; \omega_d) = \frac{(c_i^\mu)^2}{D} (E_\mu \approx E) = \frac{1}{2\pi} \frac{\Gamma^\downarrow}{(\omega_d - E)^2 + [\Gamma^\downarrow/2]^2}. \quad (18)$$

Here, the spreading width $\Gamma^\downarrow = 2\pi\sigma^2/D$ is determined by the local density of two-phonon states $\rho_{\text{two-phonon}}(E_\mu \approx E) = 1/D$. As before, σ is the average coupling strength.

Before we proceed further, there are a few comments in order. First, with the increase of the excitation energy the density of two-phonon states is increasing. Second, the coupling matrix elements strongly fluctuate (see, e.g., Fig. 5 in Ref. [26]). However, it was shown in Refs. [26,31] that the PPC matrix elements, following a Gaussian distribution or a truncated Cauchy distributions, produce the same final spreading of the $B(E1)$ strength in the doorway model, provided the root-mean-square values σ of the matrix elements (a constant for a chosen nucleus) are the same. We recall that in the full microscopic calculations the two-phonon energies are calculated by the coupling of the corresponding two one-phonon energies, each obtained in the QRPA calculations. The cumulative density of two-phonon states for ^{206}Hg and ^{210}Po is shown in Fig. 2. In the next subsection we derive a simple expression for the density of two-phonon states composed of one-phonon states, utilizing Fermi-type level densities.

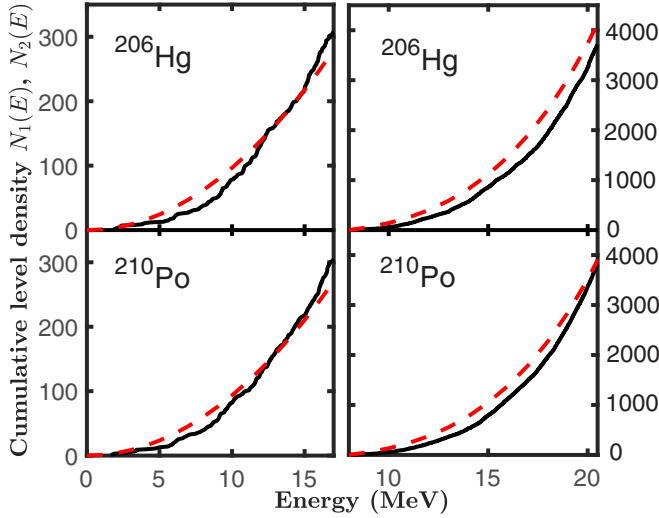


FIG. 2. Cumulative level densities of one-phonon, $N_1(E)$ (top and bottom, left-hand scale), and two-phonon, $N_2(E)$, states (top and bottom, right-hand scale) of ^{206}Hg (top) and ^{210}Po (bottom). All one-phonon states with 0^+ , 1^- , 2^+ , 3^- , and 4^+ are included. The two-phonon states are coupled to the angular momentum 1^- . Results from the QRPA calculations are shown by solid black lines, and those from the Fermi gas model are shown by dashed red lines.

1. Density of two-phonon states

Before describing the density of two-phonon states in a simple model, we start our discussion from the one-phonon states.

We assume that mean-field proton (neutron) single-particle energies are uniformly spaced in the vicinity of the Fermi surface with a spacing constant $\varepsilon=1/g$. For the considered nuclei we get $\varepsilon_p \approx \varepsilon_n \approx 0.29$ MeV from the states in the energy range of 8 MeV around the Fermi surface for protons as well as for neutrons, where the effective mass $m^*/m=0.7$ in the SLy4 Skyrme interaction is accounted for. A small value of g , or a small value of the level-density parameter $a=\pi^2(g_p + g_n)/6 = \pi^2 g/3=11.3$ MeV $^{-1}$, is expected for nuclei around ^{208}Pb (e.g., Ref. [32]). If states more distant to the Fermi surface are accounted for, corresponding to higher excitation energies, a smaller ε value appears.

We suppose that one-phonon states are constructed from proton and neutron contributions on an equal footing, which implies a factor 2 in the level density. Additionally, a factor 1/2 comes from the assumption of equal contribution from each parity. Consequently, the energy dependence of the density of one-phonon states with an angular momentum I and a parity π can be expressed as

$$\rho_{\text{one-phonon}}(I^\pi, E) = \frac{1}{2} F(I, T) 2g^2 E, \quad (19)$$

where the density of one-phonon states is approximated by the density of one-particle–one-hole states with a given spin and parity (see for details Ref. [33], and also the textbook [34]). The factor $F(I, T)$ describes the fraction of angular momentum I states. Assuming a random coupling of angular momenta at a temperature T , one arrives to the distribution

function:

$$F(I, T) = \frac{2I + 1}{2\sigma_T^2} \exp\left[-\frac{I(I+1)}{2\sigma_T^2}\right] \quad (20)$$

with the spin cutoff parameter $\sigma_T^2 = J_{\text{rig}} T / \hbar^2$. Here, $J_{\text{rig}} = A^{5/3} / 72$ MeV, is the moment of inertia of a rigid body with the same density distribution as the nucleus. The latter assumption is well justified by the study of shell correction behavior at high excitation energies [35].

We are interested in two-phonon states as background states for the GDR states populated around 14 MeV. A typical one-phonon energy that contributes to the formation of the two-phonon energies is thus $U \approx 7$ MeV. It results in the temperature value $T = \sqrt{U/a} \approx 0.79$ MeV, and spin cutoff parameters $\sigma_T \approx 8.8$ and 9.0 for ^{206}Hg and ^{210}Po , respectively. These values are adopted for the statistical description of the distribution (20).

To test the validity of these approximations we study the energy dependence of the one-phonon level density. To improve the statistics all QRPA calculated one-phonon states with 0^+ , 1^- , 2^+ , 3^- , and 4^+ are added. The corresponding one-phonon level density becomes in the Fermi gas model

$$\rho_{\text{one-phonon}}(E) = \sum_{I=0}^4 \rho_{\text{one-phonon}}(I^\pi, E). \quad (21)$$

The cumulative densities

$$N_1(E) = \int_0^E \rho_{\text{one-phonon}}(E') dE' \quad (22)$$

are shown for ^{206}Hg and ^{210}Po in Fig. 2 (top and bottom left-hand scale, respectively). The comparison of the Fermi gas results with the microscopic QRPA results demonstrates the excellent agreement.

Taking into account the above arguments, we define that the coupling of two phonons with angular momenta $I_1^{\pi_1}$ and $I_2^{\pi_2}$ to angular momentum I determines the density of two-phonon states with energy E as

$$\begin{aligned} \rho_{\text{two-phonon}}(I, E) &= \int_0^E \rho_{\text{one-phonon}}(I_1^{\pi_1}, e) \rho_{\text{one-phonon}}(I_2^{\pi_2}, E - e) de \\ &= \frac{1}{6} g^4 E^3 F(I_1, T) F(I_2, T). \end{aligned} \quad (23)$$

We recall that in the PPC model the two-phonon states with 1^- are built from the phonons with $I^\pi = 0^+, 1^-, 2^+, 3^-$, and 4^+ . Correspondingly, in the simple model we have

$$\begin{aligned} \rho_{\text{two-phonon}}(1^-, E) &= \frac{1}{6} g^4 E^3 \sum_{j=0}^3 F(j, T) F(j+1, T) \\ &\equiv \frac{1}{6\varepsilon^4} E^3 S(T). \end{aligned} \quad (24)$$

From Eqs. (20) and (24) we obtain $S(T)=0.0041$ and 0.0038 for ^{206}Hg and ^{210}Po , respectively. Thus, Eq. (24) describes the selection of angular momentum 1^- states from the considered one-phonon combinations in the neighborhood of the centroid location of the GDR.

In Fig. 2 (top and bottom, right-hand scale) the cumulative level density of the two-phonon 1^- spectrum, obtained within the QRPA in the energy interval 8–20.5 MeV, is compared to the cumulative version of Eq. (24):

$$N_2(E) = \frac{S(T)}{6\epsilon^4} \int_{E_1}^E E'^3 dE' = \frac{1}{24\epsilon^4} (E^4 - E_1^4) S(T). \quad (25)$$

The remarkable agreement between the QRPA calculated level densities and the level densities, calculated in the simple models (see Fig. 2), guides us to the following proposal, discussed below.

2. Dipole strength distribution

We recall that the results, obtained within the doorway model, are based on the assumption that it is enough to generate the one-phonon GDR states with a good accuracy within the microscopic approach, while the background states as well as the coupling matrix elements can be replaced by random matrix elements of the GOE type. Note also that the results, obtained within the PPC and the doorway model, demonstrate evidently that the background states can be treated perturbatively, since the decay is basically due to the Landau damping. In this case the RPA approach should provide the reliable description of the spreading width. In virtue of the results discussed above, we suggest (i) to use only the microscopic one-phonon states of the dipole nature and (ii) to mimic the background states with the aid of the Fermi gas model with the density (24). We recall that in the PPC calculations the energy interval for the location of the resonance width is defined by the fulfillment of the energy-weighted sum rule, symmetrically around the centroid's position (E_c), giving $E_1 = 8$ MeV and $E_{\max} = 20.5$ MeV for the nuclei here considered. States outside of this energy interval do not contribute to the GDR strength function. Consequently, it is natural to choose the same approach and the same interval for the hybrid model.

Following the above proposal, we simulate the dipole strength distribution $b(E1; E)$ without the numerical diagonalization (13), only on the basis of the one-phonon transitions (15):

$$b(E1; E) = \int_{E_1}^{E_{\max}} b^d(E1; x) f(\tilde{E}; x) dx = \sum_{i=1}^{N_d} |B_i|^2 f(\tilde{E}; E_i), \quad (26)$$

folded by the energy-dependent Lorentzian

$$f(\tilde{E}, x) = \frac{1}{2\pi} \frac{\Gamma^\downarrow(x)}{(\tilde{E} - x)^2 + [\Gamma^\downarrow(x)/2]^2}. \quad (27)$$

Due to the interaction with the two-phonon background states, the one-phonon energies $x \equiv E_i$ are shifted in energy: $\tilde{E} - x \Rightarrow E - (E_i - \Delta E)$. The spreading width

$$\Gamma^\downarrow(x) = 2\pi\sigma^2\rho_{\text{two-phonon}}(x), \quad (28)$$

where the density $\rho_{\text{two-phonon}}(x)$ is defined by Eq. (24).

From these equations it follows that in our approach $\Gamma^\downarrow \sim E^\beta$, where $\beta=3$. We recall that in the Lorentzian model [36] it was found that the value $\beta=3.5$ gives a satisfactory description of experimental data in ^{208}Pb . In a way, our results (26)–(28) for near-spherical nuclei around ^{208}Pb are in a close

correspondence with the Lorentzian model, while the two approaches have different backgrounds.

The energy shift ΔE depends on energy and can be approximated by the second-order term of the perturbation theory if we assume a weak interaction σ between the one-phonon state and the background of two-phonon states:

$$\Delta E(E) = \int_{E_1}^{E_{\max}} \frac{\sigma^2 \rho_{\text{two-phonon}}(x)}{x - E} dx, \quad E_1 < E < E_{\max}. \quad (29)$$

Here, the energy variable E corresponds to the unperturbed one-phonon energy. Taking into account Eq. (24), the integration (29) leads us to the following result for the energy shift:

$$\Delta E(E) = \frac{\sigma^2 S(T)}{6\epsilon^4} \left[\frac{1}{3} (E_{\max}^3 - E_1^3) + \frac{1}{2} E (E_{\max}^2 - E_1^2) + E^2 (E_{\max} - E_1) + E^3 \ln \left(\frac{E_{\max} - E}{E - E_1} \right) \right]. \quad (30)$$

It should be pointed out that the validity of our approximation is based on the fact that one-phonon states do not overlap, and each of them can be treated separately.

Although our results are obtained by simple means, similar results for the dipole strength distribution have been derived in the extended RPA theory in the diagonal approximation with respect to the RPA states [37]. In addition to the difference between the methods used in both approaches, there is a difference in the energy argument of the width $\Gamma^\downarrow(x)$. In Ref. [37] the variable x is the energy variable, while in our approach it is the one-phonon energy E_i . However, the root of differences becomes obvious, if we apply the ideas of the doorway model, Eqs. (9) and (12), to the definition of the width of the RPA one-phonon state ($1ph$) of Ref. [37]:

$$\begin{aligned} \Gamma^\downarrow(\omega) &= 2\pi \sum_{2p2h} |(1ph|V|2p2h)|^2 \delta(\hbar\omega - \epsilon_{2p2h}) \\ &\approx 2\pi\sigma^2 \rho_{2p2h}(\epsilon_{2p2h}) \Rightarrow \omega \equiv \epsilon_{2p2h}. \end{aligned}$$

Here, the variable σ is the rms value of the interaction between the very collective RPA state and two particle-two hole ($2p2h$) states, and $\rho_{2p2h}(\epsilon_{2p2h})$ is the local density of $2p2h$ states.

The energy shift (30) for ^{210}Po is shown in Fig. 3 for the energy interval 9.5–18.5 MeV. This energy range corresponds to the interval, taken for the calculations of the integral characteristics in Table I. For the sake of illustration we use the continuous variable E . For most states the energy shift is positive; they are pushed down in energy due to the interaction with higher-lying states. However, due to the energy cutoff at E_{\max} the energy shift is negative for the highest energies considered.

Additionally to results displayed in Fig. 1 for ^{206}Pb , we compare the results for the dipole strength for two $N=126$ isotones ^{206}Hg and ^{210}Po , obtained in the QRPA [see Figs. 4(a) and 4(d)], with the microscopic coupling [see Figs. 4(b) and 4(e)], and within the doorway and hybrid models for ^{210}Po and ^{206}Hg [compare Figs. 4(c) and 4(f)]. Evidently, the results are very similar in all considered cases (see also Table I). We recall, however, that it is required to average over a few realizations of the random interaction in the doorway model to

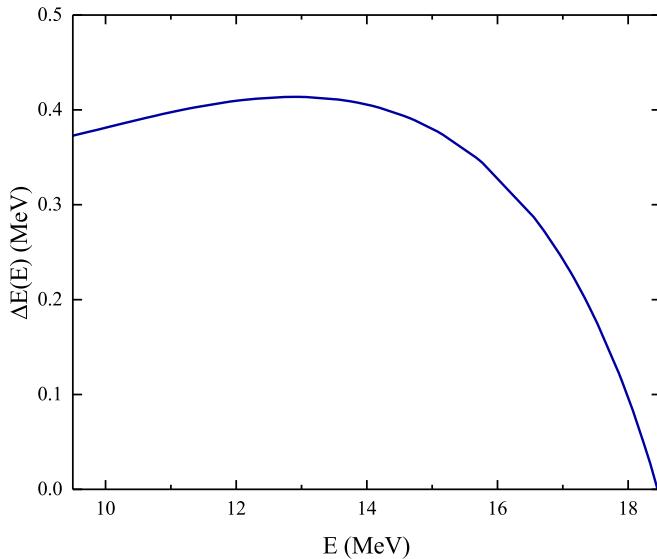


FIG. 3. Energy shift $\Delta E(E)$ [Eq. (30)] vs energy, E , for ^{210}Po with $E_1 = 8$ MeV and $E_{\text{max}} = 20.5$ MeV.

obtain the agreement with the PPC. In contrast, it is enough to calculate the strength distribution once and only once within the hybrid model. After all, we obtain a very close agreement with the results of the doorway model. Comparing the results for the hybrid model without ($\Delta E = 0$) and with the energy shift ($\Delta E \neq 0$), we find that the main peak of the GDR strength distribution moves down in energy by about 400 keV in the latter case [see Figs. 1(c), 4(c), and 4(f)]. In total, the energy shift (30) yields a perceptible change in the redistribution of the dipole strength.

C. Concluding remarks

The hybrid model provides a simplified analytical solution for the spreading width Γ^\downarrow , avoiding the full microscopic PPC calculations. The calculation procedure can be divided into the following steps.

- (1) Energies and transition matrix elements of the GDR one-phonon states are calculated in the QRPA.
- (2) The level density of two-phonon states, considered as background states, is described by Eq. (24), where the parameter ε is determined from the single-particle states around the Fermi surface (accounting for the effective mass).
- (3) The coupling strength σ , Eq. (12), may be obtained from the following considerations.

We recall that, varying the coupling strength between the one-phonon and the two-phonon states, the degree of complexity (chaoticity) is changed. In Ref. [26] it was found that the coupling strength can be determined from the condition $\sigma = \sigma_{\text{rand}}$, where σ_{rand} is the coupling strength where chaos sets in (measured in terms of spectrum fluctuations).

With the assumption $\sigma = \sigma_{\text{rand}}$, we have obtained the following results for σ_{rand} : 24 keV for ^{210}Po and ^{206}Hg and 20 keV for ^{206}Pb .

- (4) Alternatively, a simple estimation of the strength parameter σ may be done in the following way. Our analysis shows that the PPC results as well as those obtained by means of the doorway model manifest about $\approx 10\%$ increase of the decay width in comparison to the one-phonon prediction, i.e., $\Gamma^\downarrow \approx 0.1\Gamma_L$; see Table I. This result guides us to suppose that the parameter σ can be estimated from Eqs. (24) and (28), assuming that the values E_c and Γ_L are calculated within the standard QRPA. As an example, for ^{206}Pb we obtain $\sigma \approx 18$ keV, which is not too far from the random value $\sigma_{\text{rand}} = 20$ keV.
- (5) The energy-dependent energy shift, $\Delta E(E)$, is calculated from Eq. (30). Finally, the dipole strength distribution is obtained from Eq. (26).

IV. SUMMARY

The results for decay widths of the GDR in heavy nuclei around ^{208}Pb have been obtained in the one-phonon approximation and in the PPC approach, in the framework of the microscopic model (see details in Ref. [26]). The comparison of these results demonstrates that the Landau damping shows up as the basic mechanism of the decay. Our analysis confirms as well that the influence of the PPC is much more prominent on the strength redistribution, while it is less important for the location of the resonance energy centroid. Further, we confirm that the calculations, in which the doorway microscopic one-phonon 1^- states interact randomly with the background two-phonon states of the GOE type, are also in a good agreement with the PPC results for the considered nuclei. These results give us impetus to simplify drastically the description of the dipole strength distribution by considering microscopically only one-phonon states.

We found that fragmentation and the redistribution of the one-phonon states can be reproduced with the aid of the energy-dependent Lorentzian function (27). This energy dependence is brought about by the energy-dependent one-phonon width $\Gamma^\downarrow(E)$ and the energy shift $\Delta E(E)$. In the definition of these variables the crucial role is played by the *two-phonon density*, provided by the Fermi gas model with uniformly spaced states with a constant spacing that mimics the background states. The comparison of the results for the spreading width of the GDR, obtained within the hybrid and the doorway model, demonstrates as well a good agreement (see Figs. 1 and 4 and Table I).

The hybrid model can be extended to include the coupling of other types of phonons like magnetic phonons and phonons with higher angular momenta. And, in principle, also background states of three-phonon character can be accounted for. It should be noted as well that the ground state correlations beyond the RPA [38,39] may play an important role. In this context the problem of convergence and stability of solutions of the beyond RPA models [40] and the so-called problem of double counting [41] have been discussed recently. However, all these questions are beyond the scope of the present paper, and require separate studies.

Thus, the analytically solvable hybrid model enables us to overcome the difficulty of microscopic calculations of the

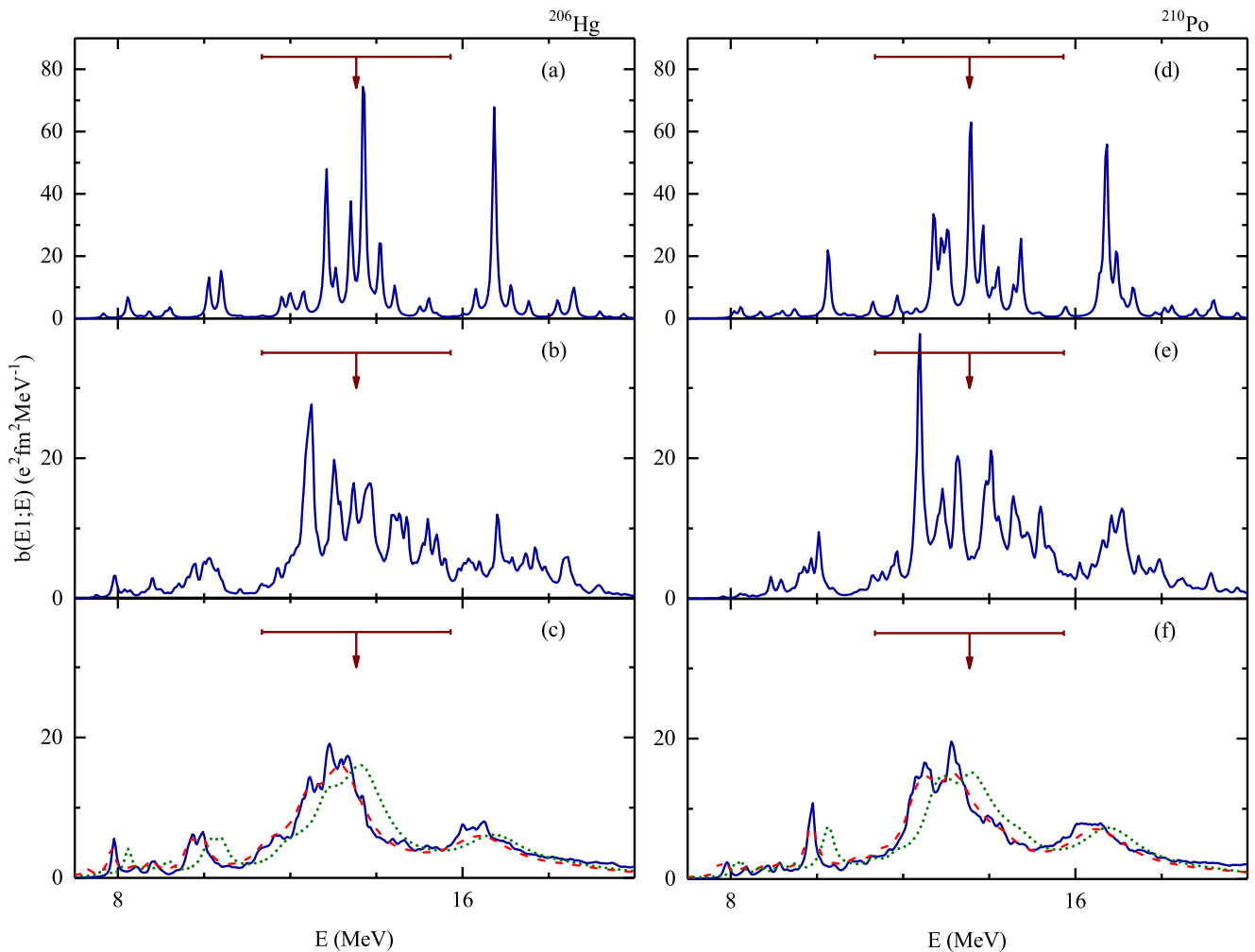


FIG. 4. Similar to Fig. 1, for ^{206}Hg (left panels) and ^{210}Po (right panels). The empirical systematics of the centroid energy and width are denoted by arrows and lines in panels (a)–(f), respectively.

dipole decay evolution through the sequence of the complex configurations to compound states. This model might be useful for an efficient description of the decay width of the GDR in heavy nuclei, once the calculation of the microscopic one-phonon states is done in the RPA (QRPA). It seems reasonable to conjecture that the proposed approach could be useful as well for other microscopic models of spreading width of the GDR, where the application of the RPA (QRPA) approach is well justified.

ACKNOWLEDGMENTS

A.P.S. is thankful for the hospitality at the Division of Mathematical Physics, Lund University, where a part of this work has been done. S.Å. thanks the Swedish Natural Science Research Council for financial support, and the Bogoliubov Laboratory of Theoretical Physics for warm hospitality. This work was partially supported by the National Research Foundation of South Africa, Grant No. 129603.

- [1] M. Arnould and S. Goriely, *Prog. Part. Nucl. Phys.* **112**, 103766 (2020).
- [2] F. Özel and P. Freire, *Annu. Rev. Astron. Astrophys.* **54**, 401 (2016).
- [3] H. Yasin, S. Schäfer, A. Arcones, and A. Schwenk, *Phys. Rev. Lett.* **124**, 092701 (2020).
- [4] X. Roca-Maza and N. Paar, *Prog. Part. Nucl. Phys.* **101**, 96 (2018).

- [5] A. Bohr and B. M. Mottelson, *Nuclear Structure* (Benjamin, New York, 1969), Vol. 1.
- [6] A. B. Migdal, *J. Phys. Acad. Sci. USSR* **8**, 331 (1944); *J. Exp. Theor. Phys. USSR* **15**, 81 (1945).
- [7] A. Bohr and B. M. Mottelson, *Nuclear Structure* (Benjamin, New York, 1975), Vol. 2.
- [8] G. F. Bertsch, P. F. Bortignon, and R. A. Broglia, *Rev. Mod. Phys.* **55**, 287 (1983).

- [9] V. G. Soloviev, *Theory of Atomic Nuclei: Quasiparticles and Phonons* (Institute of Physics, University of Reading, Berkshire, 1992).
- [10] S. Kamezdzhiev, J. Speth, G. Tertychny, and V. Tselyaev, *Nucl. Phys. A* **555**, 90 (1993).
- [11] N. Paar, D. Vretenar, E. Khan, and G. Colò, *Rep. Prog. Phys.* **70**, 691 (2007).
- [12] S. Goriely, P. Dimitriou, M. Wiedeking, T. Belgya, R. Firestone, J. Kopecky, M. Krtička, V. Plujko, R. Schwengner, S. Siem, H. Utsunomiya, S. Hilaire, S. Péru, Y. S. Cho, D. M. Filipescu, N. Iwamoto, T. Kawano, V. Varlamov, and R. Xu, *Eur. Phys. J. A* **55**, 172 (2019).
- [13] P. von Neumann-Cosel and A. Tamii, *Eur. Phys. J. A* **55**, 110 (2019).
- [14] H. Aiba and M. Matsuo, *Phys. Rev. C* **60**, 034307 (1999).
- [15] D. Lacroix and P. Chomaz, *Phys. Rev. C* **60**, 064307 (1999); **62**, 029901(E) (2000).
- [16] W. D. Heiss, R. G. Nazmitdinov, and F. D. Smit, *Phys. Rev. C* **81**, 034604 (2010).
- [17] I. Hamamoto, H. Sagawa, and X. Z. Zhang, *Phys. Rev. C* **57**, R1064(R) (1998).
- [18] V. Tselyaev, N. Lyutorovich, J. Speth, S. Krewald, and P.-G. Reinhard, *Phys. Rev. C* **94**, 034306 (2016).
- [19] N. Lyutorovich, V. Tselyaev, J. Speth, and P.-G. Reinhard, *Phys. Rev. C* **98**, 054304 (2018).
- [20] N. Van Giai, Ch. Stoyanov, and V. V. Voronov, *Phys. Rev. C* **57**, 1204 (1998).
- [21] A. P. Severyukhin, V. V. Voronov, and N. Van Giai, *Phys. Rev. C* **77**, 024322 (2008).
- [22] E. Chabanat, P. Bonche, P. Haensel, J. Meyer, and R. Schaeffer, *Nucl. Phys. A* **635**, 231 (1998); **643**, 441(E) (1998).
- [23] A. P. Severyukhin, V. V. Voronov, and N. Van Giai, *Eur. Phys. J. A* **22**, 397 (2004).
- [24] A. P. Severyukhin, N. N. Arsenyev, and N. Pietralla, *Phys. Rev. C* **86**, 024311 (2012).
- [25] A. P. Severyukhin, S. Åberg, N. N. Arsenyev, and R. G. Nazmitdinov, *Phys. Rev. C* **95**, 061305(R) (2017).
- [26] A. P. Severyukhin, S. Åberg, N. N. Arsenyev, and R. G. Nazmitdinov, *Phys. Rev. C* **98**, 044319 (2018).
- [27] S. Goriely and V. Plujko, *Phys. Rev. C* **99**, 014303 (2019).
- [28] B. L. Berman and S. C. Fultz, *Rev. Mod. Phys.* **47**, 713 (1975).
- [29] E. Lipparini and S. Stringari, *Phys. Rep.* **175**, 103 (1989).
- [30] S. Adachi and N. Van Giai, *Phys. Lett. B* **149**, 447 (1984).
- [31] A. P. Severyukhin, S. Åberg, N. N. Arsenyev, and R. G. Nazmitdinov, *Phys. Rev. C* **97**, 059802 (2018).
- [32] W. Dilg, S. Schantl, H. Vonach, and M. Uhl, *Nucl. Phys. A* **217**, 269 (1973).
- [33] F. C. Williams, Jr., *Nucl. Phys. A* **166**, 231 (1971).
- [34] A. V. Ignatyuk, *Statistical Properties of Excited Atomic Nuclei* (Energoizdat, Moscow, 1983).
- [35] A. V. Ignatyuk, I. N. Mikhailov, L. H. Molina, R. G. Nazmitdinov, and K. Pomorsky, *Nucl. Phys. A* **346**, 191 (1980).
- [36] C. B. Dover, R. H. Lemmer, and F. J. W. Hahne, *Ann. Phys. (NY)* **70**, 458 (1972).
- [37] J. Wambach, *Rep. Prog. Phys.* **51**, 989 (1988).
- [38] V. V. Voronov, D. Karadjov, F. Catara, and A. P. Severyukhin, *Fiz. Elem. Chastits At. Yadra* **31**, 905 (2000) [*Phys. Part. Nucl.* **31**, 452 (2000)].
- [39] M. Tohyama, *Phys. Rev. C* **87**, 054330 (2013).
- [40] P. Papakonstantinou and R. Roth, *Phys. Rev. C* **81**, 024317 (2010).
- [41] V. I. Tselyaev, *Phys. Rev. C* **88**, 054301 (2013).